

Influence of geometry on positron binding to molecules

J R Danielson^{*} , S Ghosh  and C M Surko 

Department of Physics, University of California San Diego, La Jolla, CA 92093, United States of America

E-mail: jrdanielson@ucsd.edu, soumen@physics.ucsd.edu and csurko@ucsd.edu

Received 1 September 2021, revised 10 November 2021

Accepted for publication 30 November 2021

Published 22 December 2021



CrossMark

Abstract

Annihilation studies have established that positrons bind to most molecules. They also provide measurements of the positron-molecule binding energies, which are found to vary widely and depend upon molecular size and composition. Trends of binding energy with global parameters such as molecular polarizability and dipole moment have been discussed previously. In this paper, the dependence of binding energy on molecular geometry is investigated by studying resonant positron annihilation on selected pairs of isomers. It is found that molecular geometry can play a significant role in determining the binding energies even for isomers with very similar polarizabilities and dipole moments. The possible origins of this dependence are discussed.

Keywords: slow positron beam, positron–molecule bound states, positron binding energy, molecular geometry, isomers, dipole moment

(Some figures may appear in colour only in the online journal)

1. Introduction

Studies of resonant positron annihilation on molecules provide evidence that positrons bind to most polyatomic molecular targets. The energies of these resonances provide a direct measure of the positron-molecule binding energy [1]. Data are now available for over eighty molecules. There has also been much progress in understanding these bound states theoretically. Although results from *ab initio* calculations are often quite dependent on the exact technique used, there have been several recent calculations for molecules with large dipole moments have been able to predict binding energies to within 30% of the measurements [2, 3]. Further, a new many-body approach to calculate the positron-molecule correlation energies has resulted in unprecedented agreement ($\sim 1\%$) with measured binding energies for several molecules [4]. It also provides new insights into the effect of virtual positronium formation and identifies the role of specific molecular orbitals in determining binding energies. However, it comes with a high computational cost.

Refined effective potential models have also produced important insights into positron–molecule binding [5–11]. In this case, the correlation interaction is approximated using a model potential that contains a number of parameters that are determined by fitting to the binding energy of one or a few molecules. This necessitates having at least one measurement or high-quality calculation in order to perform the fit, and thus these models are most useful for families of molecules that contain similar bonds (e.g. alkane chains [5] or chloro-alkanes [11]). Although the model potentials are necessarily approximate and sensitive to the fit parameters, the results of these calculations are enabling new insights, such as visualization of the extended positron bound-state wave function, at a low computational cost. Further, these models use the calculated shapes of the molecules and so they also exhibit the important effects of the molecular geometry on positron binding. This is in agreement with the conclusions of the work presented here.

Alternatively, phenomenological models have also been constructed using global molecular parameters (e.g. permanent dipole moment, molecular polarizability and the number of π bonds) to predict binding energies [12–16]. Trends in binding energy can be captured for families of molecules using this approach. However, this approach may fail when

* Author to whom any correspondence should be addressed.

attempting to apply this technique to new types of molecules [17, 18].

These positron–molecule bound states have been related to analogous electron–molecule bound states (frequently referred to as ‘dipole bound states’) [19–22]. Experimentally, the binding energies of these diffuse electron states are an order of magnitude or more smaller than those of the analogous positron states [23–28]. There are two reasons for this [28]. For the typical polar molecule, the negative end of the molecular dipole is at the outer edge of the molecule, and the positron can get closer to the attractive dipole potential. In addition, new *ab initio* calculations [4] give the best support to date that the short-range positron molecule correlation potential is much stronger than the corresponding electron–molecule potential.

The work presented here explores the influence of molecular geometry on the positron binding energy. This is accomplished by comparing the measured positron–molecule binding energies for selected pairs of isomers (i.e. molecules having the same chemical composition but different arrangements of the atoms). For the molecules studied here, the parameters considered are the molecular polarizability, α , the molecular dipole moment, μ , and the molecular ionization potential, E_i , all of which are known. A simple case is that of hydrocarbon chain isomers, where a substituted atom (or group) is moved from the 1st carbon to the 2nd carbon in the chain. An example of this is 1-chloropropane as compared to 2-chloropropane, where the chlorine atom is on the first carbon (end of the chain) in the former and on the second (middle) carbon in the latter. The interesting feature of such a pair is that, since the atomic constituents do not change, the global molecular parameters are approximately the same and so the only remaining difference would appear to be the arrangement of atoms in the molecule (i.e. the geometry).

The remainder of the paper is as follows. Section 2 contains a brief description of the experimental techniques used in the binding energy measurements and how the positron–molecule binding energy, ε_B , is obtained from the low-energy positron annihilation spectra as a function of incident positron energy. Comparisons of selected annihilation spectra for specific isomer pairs are also shown. The experimental results for binding energy are presented in section 3. They demonstrate the need to consider factors beyond the global molecular parameters in determining ε_B , and they specifically highlight the important role played by molecular geometry. Section 4 presents a set of concluding remarks.

2. Experimental method

The experimental techniques have been described in detail previously, and so only a brief description is presented here [1, 29, 30]. Slow positrons (\sim eV) are obtained from a ^{22}Na radioisotope source and a neon-moderator. They are magnetically guided into a three-stage buffer-gas trap [31]. The positrons lose energy via collisions with room temperature N_2 and CF_4 molecules and are accumulated in a Penning–Malmberg trap [32]. After cooling to room temperature, the positrons are gently ejected from the trap by pulsing the confining electrodes to form a nearly monoenergetic positron

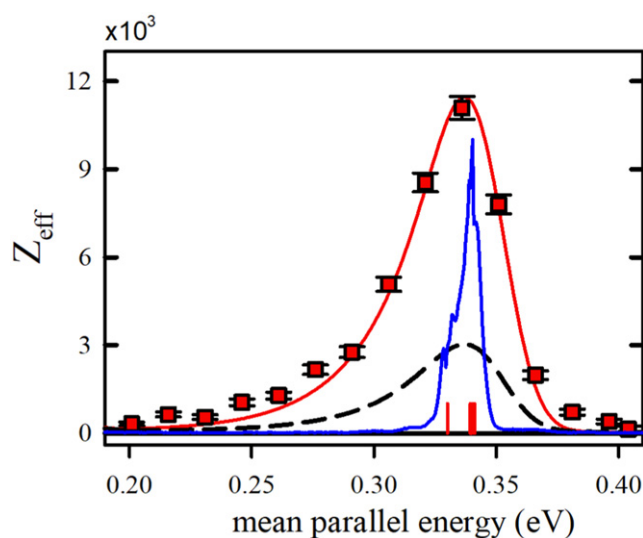


Figure 1. Measured spectrum for the normalized annihilation rate Z_{eff} for propane (red squares) as a function of the mean parallel energy of the beam in the region of the C–H stretch vibrational modes. Error bars are set by counting statistics. The energy axis here corrects a shift in the original data published in [29]. Solid red line is the fit to the enhanced VFR model with $\varepsilon_B = 16 \pm 3$ meV. Dashed blue curve is the unscaled GL theory curve using the same ε_B . Solid blue line is the shifted IR spectrum (from reference [36], arbitrary linear scale with the peak set to 10 000). Vertical lines show shifted positions of the dipole active fundamental modes. See text for details.

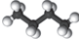
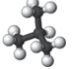
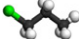
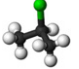
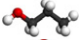
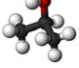
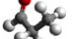
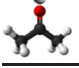
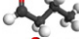
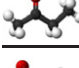

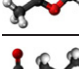
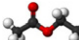

beam [30]. The beam is ~ 0.5 cm in diameter, with a temporal pulse width ~ 2 μs and energy spread < 40 meV FWHM. The mean energy of the beam out is controllable and set to ~ 0.7 eV for most of the experiments described here. The typical number of positrons is ~ 20 000, but this can be varied depending on the experiment.

The positron pulse is magnetically guided into a gas cell where an electrode is electrically biased to control the mean energy of the beam. The test gas is injected into the gas cell through a leak valve. The 300 K test gas is maintained in the pressure range of 1–30 μtorr (depending on the molecule), as measured with a manometer. Annihilation gamma rays are measured while the beam interacts with the test gas. The beam energy distribution is measured using a retarding potential analyzer [1, 30, 33]. The count rate vs positron energy is converted into a normalized annihilation rate Z_{eff} [29] using the known number of positrons per pulse, gas pressure, and detector calibration. Measurement of the annihilation as a function of the bias on the gas cell yields the annihilation rate as a function of incident positron energy.

The example of an annihilation spectrum for propane is shown in figure 1, where the vertical axis is Z_{eff} , and the horizontal axis is the measured mean parallel energy of the beam. The result is a strongly peaked, asymmetric structure near 350 meV due to the high-energy C–H stretch modes, and a second, broader structure of lower magnitude at lower energies due to C–C and C–H bend and twist modes (not shown). See references [1, 29, 30] for more details.

The Gribakin–Lee (GL) theory for positron annihilation via vibrational Feshbach resonances [1, 34] can be used to analyze

Table 1. Positron–molecule binding energies ε_B (meV) for 1- and 2-isomers, with permanent dipole moments μ (D), average static dipole polarizabilities α (\AA^3), and ionization energies E_i (eV). Values for μ and E_i are from [42], α for liquids from index of refraction data [42] and for gases from [43]. Where multiple conformers exist, average μ is listed, except for the trans–trans (TT) conformer of ethyl acetate [44]. Colored symbols green, blue, purple, cyan denote increasing values of α , respectively.

	Molecule	ε_B (meV)	μ (D)	α (\AA^3)	E_i (eV)	Sym.
	Butane (C ₄ H ₁₀)	36 ± 3	0	8.14	10.53	▲
	Isobutane (C ₄ H ₁₀)	41 ± 3	0.13	8.14	10.57	▲
	1-chloropropane (C ₃ H ₇ Cl)	97 ± 4	2.05	8.24	10.81	■
	2-chloropropane (C ₃ H ₇ Cl)	113 ± 5	2.17	8.36	10.79	■
	1-propanol (C ₃ H ₇ OH)	65 ± 5	1.57	6.70	10.18	▼
	2-propanol (C ₃ H ₇ OH)	85 ± 4	1.58	6.70	10.17	▼
	Propanal (C ₃ H ₆ O)	115 ± 5	2.72	6.34	9.96	●
	Acetone (C ₃ H ₆ O)	170 ± 5	2.88	6.41	9.70	●
	Butanal (C ₄ H ₈ O)	150 ± 5	2.72	8.28	9.84	●
	2-butanone (C ₄ H ₈ O)	205 ± 5	2.78	8.21	9.52	●
	Ethyl-formate (C ₃ H ₆ O ₂)	95 ± 5	1.93	7.02	10.61	◆
	Methyl-acetate (C ₃ H ₆ O ₂)	120 ± 5	1.72	6.96	10.25	◆
	propyl-formate (C ₄ H ₈ O ₂)	130 ± 10	1.89	8.85	10.52	◆
	Ethyl-acetate (TT) (C ₄ H ₈ O ₂)	190 ± 10	2.13	8.80	10.01	◆

the spectrum. Here, the fundamental vibrations of the molecule dipole-couple an incoming positron to the positron–molecule bound state. This happens only at resonant positron energies, E_ν , given by the mode energy, downshifted by the positron binding energy,

$$E_\nu = \hbar\omega_\nu - \varepsilon_B, \quad (1)$$

where $\hbar\omega_\nu$ is the energy of mode ν . If the vibrational modes (ω_ν) are known, this equation can be inverted to obtain ε_B [1, 29, 34]. In the relevant limit in which the width of the resonance is small compared with the energy spread of the positron beam, the shape of the resonance is determined by the energy distribution of the beam [30, 35].

To fit the measured spectrum, the known strength of the positron coupling of the dipole active vibrational modes (e.g. infra-red absorption data from the NIST Chemistry Webbook [36, 37]) are convolved with the experimental beam distribution, with the amplitude of the modes and the binding energy allowed to vary for best fit to the data [35, 38, 39]. For propane, this is shown by a solid line in figure 1. The sharpest feature in the spectrum is the rapid rise in annihilation just below

350 meV which corresponds to the high-energy C–H vibrational modes (shown by the vertical lines). The values of ε_B obtained this way are expected to be correct to ± 3 to 5 meV, depending on the details of the mode spectrum. The fit for propane yields $\varepsilon_B = 16 \pm 3$ meV, which is a more precise value than the previous measurement, $\varepsilon_B = 10 \pm 10$ meV [29, 40].

3. Results

The analysis described above was carried out for a number of molecules. This includes comparisons of three pairs of molecules with a simple 1- vs 2- geometric changes (butane vs isobutane, 1-propanol vs 2-propanol, 1-chloropropane vs 2-chloropropane); four pairs of molecules with the C=O double bonds located on either the first or second carbon in hydrocarbon chain molecules (propanal vs acetone, butanal vs 2-butanone, ethyl-formate vs methyl-acetate, propyl-formate vs ethyl-acetate); several other isomer pairs including some with dipole moments and larger alkanes with either zero or very small dipole moments (hexane vs 2,3-dimethylbutane, 1,3-dichloropropane vs 2,2-dichloropropane). Older data was

Table 2. Positron–molecule binding energies ε_B (meV) and relevant molecular parameters for other selected isomer pairs. Symbols and notation are the same as in table 1. See text for details.




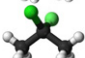




Molecule	ε_B (meV)	μ (D)	α (\AA^3)	E_i (eV)	Sym.
 Hexane (C_6H_{14})	93 ± 3	0	11.83	10.13	\blacktriangle
 2,3-dimeth.but. (C_6H_{14})	94 ± 5	0	11.81	10.02	\blacktriangle
 1,3-dichl.prop. ($\text{C}_3\text{H}_6\text{Cl}_2$)	85 ± 10	2.08	10.08	10.89	\blacksquare
 2,2-dichl.prop. ($\text{C}_3\text{H}_6\text{Cl}_2$)	130 ± 5	2.20	10.37	—	\blacksquare

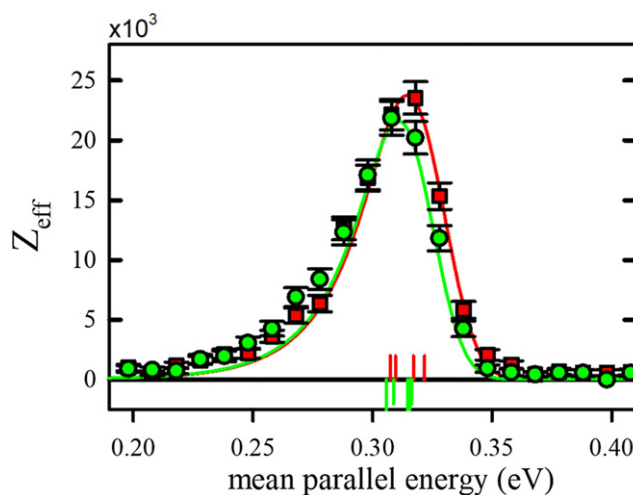
Table 3. Positron–molecule binding energies ε_B (meV) and relevant molecular parameters for chain alkane molecules. Symbols and notation are the same as in table 1.

Molecule	ε_B (meV)	μ (D)	α (\AA^3)	E_i (eV)	Sym.
 Propane (C_3H_8)	16 ± 3	0.084	6.29	10.95	\blacktriangle
 Butane (C_4H_{10})	36 ± 3	0	8.14	10.53	\blacktriangle
 Pentane (C_5H_{12})	65 ± 3	0	9.98	10.28	\blacktriangle
 Hexane (C_6H_{14})	93 ± 3	0	11.83	10.13	\blacktriangle

reanalyzed as described above in order to obtain consistent comparisons between all of the molecules. In most cases the difference with the older values is <5 meV. The data are summarized in tables 1–3, where the molecular parameters are tabulated along with the measured values of ε_B . The approximate uncertainty for each measured ε_B is also given. This value is based on the uncertainty in the beam parameters and the quality of the VFR fit to the data.

For the alkane pairs, where the dipole moment is either zero or very small, the change in ε_B is quite small. The only comparison that shows a measurable difference is butane vs isobutane, which is shown in figure 2. Here, the difference in ε_B is ~ 5 meV, with isobutane more deeply bound (i.e. the spectrum shifted to lower energies). This is close to the limit of what can be resolved with the current measurement technique. In contrast, figure 3 shows a comparison of hexane and 2,3-dimethylbutane. Although the spectra are not quite identical, the shift between the two is less than 2 meV, which is smaller than the uncertainty in the energy scale. Only a few alkane isomers have been measured, and so it is uncertain as to whether this is a generic feature of the larger alkanes. This will be discussed further below.

For pairs of isomers with a significant dipole moment, the separation in ε_B is much larger. One example, shown in figure 4, is the comparison between 1-chloropropane ($\varepsilon_B = 97$ meV) and 2-chloropropane ($\varepsilon_B = 113$ meV). The two spectra are quite similar, but 2-chloropropane is shifted to lower energy by 16 meV. This equates to roughly a 15% change of the value of ε_B when the chlorine is moved from the first (end) carbon to the second (middle) carbon. Recently, an effective potential model was used to calculate the binding energies for these molecules. The results are $\varepsilon_B \sim 95$ and 123 meV, respectively [11], in good agreement with the

**Figure 2.** Analysis of the annihilation spectrum for butane (red squares) and isobutane (green circles). Solid lines are the fits to the enhanced VFR model, yielding $\varepsilon_B = 36 \pm 3$ and $\varepsilon_B = 41 \pm 3$ meV, respectively. Vertical lines show shifted positions of the dipole active fundamental modes. Error bars are set by counting statistics.

experimental values. As shown in the table below, this difference is a common feature seen in all molecule pairs—the molecule with the substitution located nearer the molecular center is more deeply bound.

Figure 5 compares the annihilation spectra of acetone and propanal. The dipole moments of these molecules are significantly larger than those in the chloropropanes, and the difference in ε_B is much larger as well. In this case, the positron is more deeply bound to acetone by more than 50 meV, which is a 45% increase over propanal. The effect of the change in the geometry is generally larger for molecules with larger dipole moments.

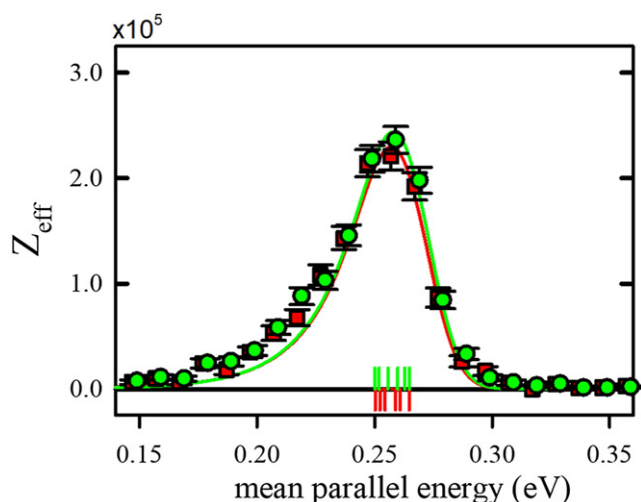


Figure 3. Analysis of the annihilation spectrum for hexane (red squares) and 2,3-dimethylbutane (green circles). Solid lines are the fits to the enhanced VFR model, yielding $\varepsilon_B = 93 \pm 3$ and $\varepsilon_B = 94 \pm 5$ meV, respectively. Vertical lines show shifted positions of the dipole active fundamental modes. Error bars are set by counting statistics.

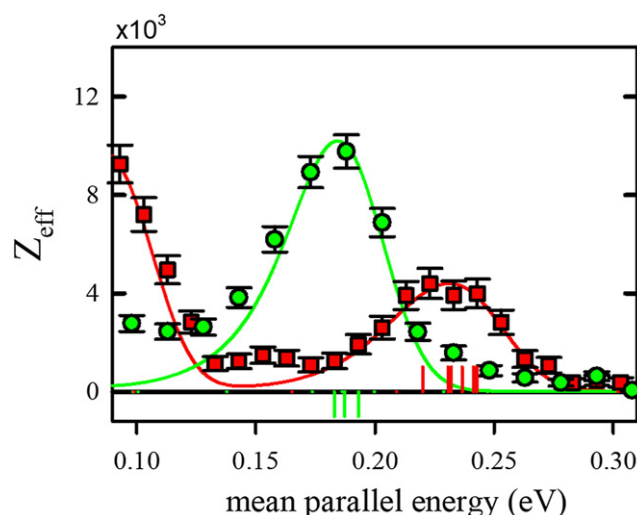


Figure 5. Analysis of the annihilation spectrum for propanal (red squares) and acetone (green circles). The energy axis here corrects a small shift in the original data published in [41]. Solid lines are the fits to the enhanced VFR model, yielding $\varepsilon_B = 115 \pm 5$ and $\varepsilon_B = 170 \pm 5$ meV, respectively. Vertical lines show shifted positions of the dipole active fundamental modes. Error bars are set by counting statistics.

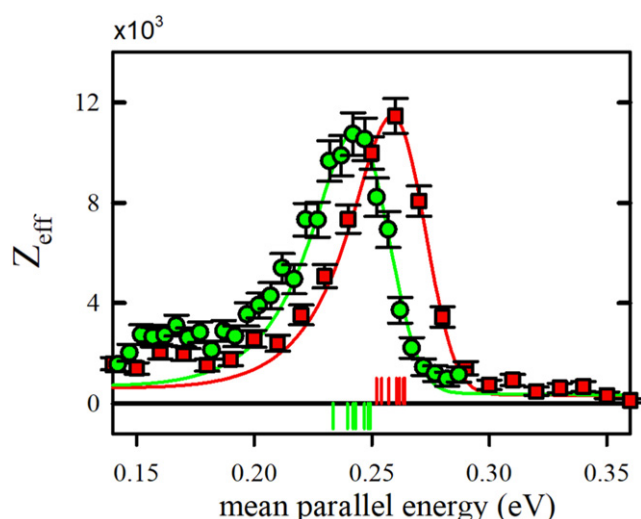


Figure 4. Analysis of the annihilation spectrum for 1-chloropropane (red squares) and 2-chloropropane (green circles). Solid lines are the fits to the enhanced VFR model yielding $\varepsilon_B = 97 \pm 4$ and $\varepsilon_B = 113 \pm 5$ meV respectively. Vertical lines show shifted positions of the dipole active fundamental modes. Error bars are set by counting statistics.

As shown tables 1–3, while the molecular parameters for each isomer pair are quite similar (difference typically $\lesssim 5\%$), the differences in ε_B are fractionally much larger. A natural way to compare the molecules is by the value of the molecular polarizability (α). Thus, for example, the alkane chain pentane is included in the table to provide a comparison with the dichloropropanes. This works well for these molecules because, in this limited set, α is approximately set by the number of carbon and chlorine atoms in the molecule, and the number of hydrogen or oxygen atoms plays only a secondary role. However, the oxygen atoms do have a strong influence on the molecule dipole moment μ . To monitor these changes,

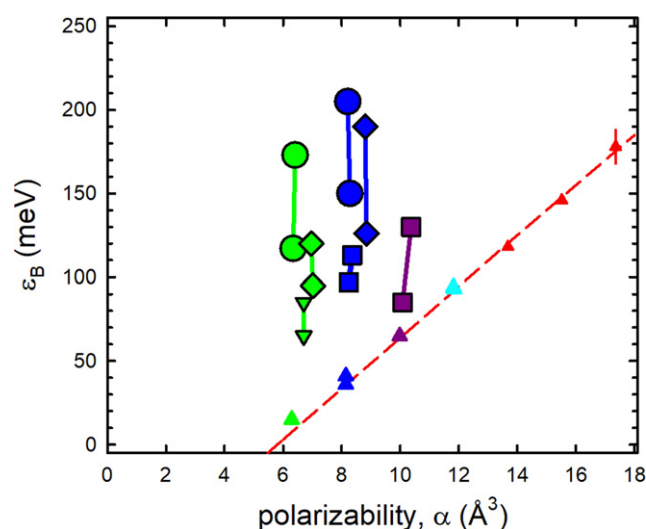


Figure 6. Measured positron binding energies, ε_B , vs the molecular polarizability, α . Up triangles (\blacktriangle) are saturated alkanes. Down triangles (\blacktriangledown) are alcohols. Circles (\bullet) are aldehydes and ketones. Diamonds (\blacklozenge) are formates and acetates. Squares (\blacksquare) are chloro-molecules. Solid lines connect isomer pairs. The colors, green, blue, purple, cyan, are in order of increasing α . Larger symbols indicate larger dipole moments. The dashed red line shows the approximate linear dependence for the chain alkanes.

the molecules will also be grouped by μ by using the size of the symbols in the plots below, where larger symbols signify larger μ .

Figure 6 shows a plot of the measured ε_B vs α for all the molecules studied here. Symbols are the same as indicated in the tables 1–3. Larger symbols indicate species with a larger dipole moment. The dashed red line shows the approximate linear dependence for the chain alkanes. The colors, green, blue, purple, cyan, are in order of increasing α , where each

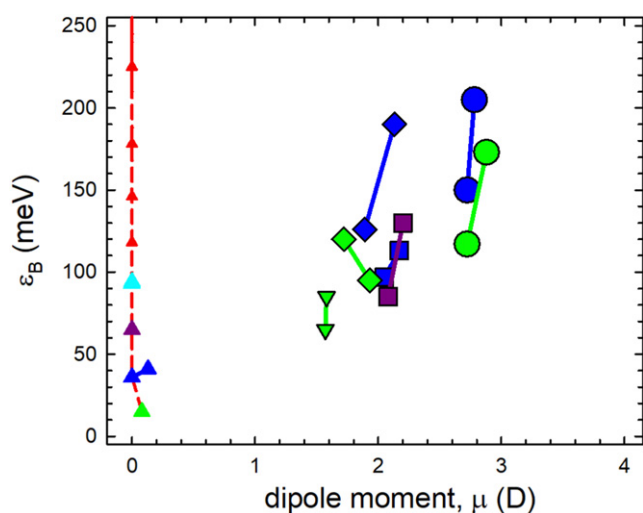


Figure 7. Measured positron binding energies, ε_B , vs the molecular dipole moment, μ . Symbol colors and notation are the same as in figure 6.

color denotes the same approximate value of α . The corresponding chain alkane has the lowest ε_B for each value of α .

As expected, figure 6 shows an increase in ε_B as α increases, but there is also a broad spread near each value of α where, in this phenomenological description, some other parameter is playing a significant role. In order to identify each pair of isomers, a solid line is used to connect the respective data points. This shows that α changes relatively little within the isomeric pairs and highlights the fact that other effects are contributing to ε_B . Generally, at fixed α , larger μ results in larger ε_B .

Previously, it was shown that a large dipole moment can lead to a significant enhancement of the positron binding energy [41], and the same result is seen for the data presented here. To investigate whether or not changes in dipole moment can explain the large differences in ε_B for the various isomer pairs, ε_B values are plotted against μ , in figure 7. Here the chain alkanes are at $\mu = 0$, with the exception of the small dipole moment for propane and isobutane. As expected, there is a general increase in ε_B with increasing μ . However, there are exceptions. The two alcohols (green down triangles) have the same dipole moment, and methyl-acetate actually has a slightly smaller dipole moment than ethyl-formate (green diamonds). In several cases, the change in the dipole moment is $\lesssim 5\%$, but ε_B changes by $\gtrsim 20\%$. Although such a strong dependence on μ is possible, it does not seem likely, nor would it explain the exceptions described above.

These results can be explained by assuming that, as the negatively charged atom (which produces the molecular dipole) moves from the first to the second carbon, the change in the geometry results in a stronger attractive dipole potential over more of the molecule. For several chlorinated molecules (including those discussed here), this effect has also been observed in two recent theory papers using effective potential methods [10, 11]. A key result from these papers is the observation that the shape and localization of the positron wavefunction is significantly altered by the changes in molecular geometry even in cases where the strength of the molecular

dipole is approximately constant [11]. Typically, more compact molecules exhibit larger values of ε_B . This feature was also observed in recent calculations for nonpolar and very weakly polar alkane conformers [6], but the difference was only appreciable (>5 meV) for molecules with six or more carbons.

It should be noted that one of the molecules in the present data set, ethyl acetate, has two components in its spectrum due to the presence of two *conformers* with different values of ε_B [17]. Previously, the difference in the dipole moment of the two conformers was used to rationalize the reason for the different ε_B . However, in light of the data presented here, it seems more likely that the difference is due to the different shapes of the conformers. This would be a good topic for study using the effective potential models described above. For simplicity, we only cite here data for the dominant conformer, which has the larger value of ε_B (see reference [17]). However, the conclusions would not change if we focused on the less prevalent conformer.

The final parameter considered here is the molecular ionization potential, E_i . In the case of positron-atom binding, E_i has been shown to be an important parameter [13, 45]. However, for the case relevant here, where the ionization potential is larger than the positronium formation energy of 6.8 eV, the polarizability and the ionization potential have an approximately inverse relationship in determining ε_B [46]. Thus, in the positron-atom case, it is possible that either term could be used to parametrize the binding energy. For molecules, however, the spatial locations of the atoms are also important. The ionization potential depends on the atoms that make up the molecule, and it is also sensitive to the bond character (e.g. single or double bond). Further, the large alkanes are a case where the ionization energy is approximately constant, but the polarizability increases with the size of the molecule.

Recently, there was a machine-learning analysis of positron binding to molecules that has argued for the importance of E_i in determining the binding energy for certain molecules with zero dipole moment [16]. It was hypothesized that this could be due to virtual positronium. The important role of virtual positronium has also been quantitatively determined in recent *ab initio* many-body calculations of positron-molecule binding energy [4]. In the latter description, many-body techniques are used to calculate the positron-electron correlation energy, including the effect of virtual positronium. For several molecules, it was found that the inclusion of virtual positronium increased the predicted binding energy by more than 50%.

To investigate possible effects related to E_i , figure 8 shows the measured ε_B vs E_i . Although the selected molecules only cover a limited range of E_i , some trends are apparent. Several sets of the isomer data lie close to the dashed red line joining the alkanes. This includes the ketones (circles) that have a large dipole moment and most of the alkane isomers. The alcohols (green triangles) are also close to the trend line, although the two have essentially the same E_i value. This could be an important trend, or it could be a coincidence. The other molecules with mid-range μ values are off the trend line; and further, the chloro molecules (squares) show very little if any change in E_i . Generally, when E_i is different for an isomer pair, ε_B increases

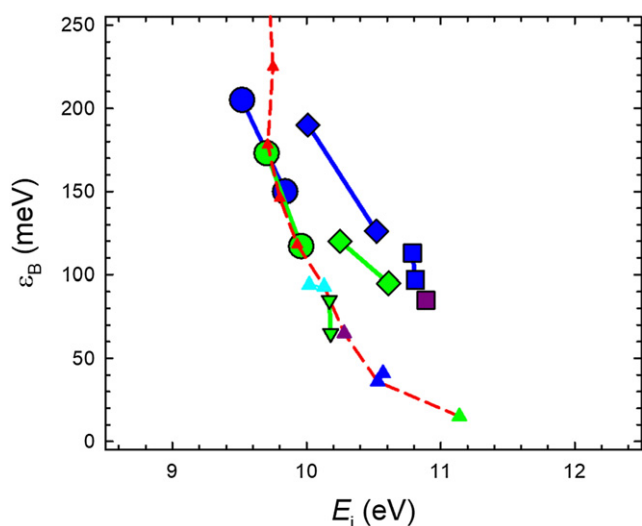


Figure 8. Measured positron binding energies, ε_B , vs the molecular ionization potential, E_i . Symbol colors and notation are the same as in figure 6. Dashed red curve connects the chain alkanes as a guide to the eye.

with decreasing E_i . The exceptions are butane and isobutane, which show the opposite behavior.

While the small selection of molecules presented here is not sufficient to make a general statement, the direct dependence of ε_B on E_i , if any, is unclear. This can be reconciled by the results of the papers discussed above that argue for the importance of virtual positronium in determining ε_B . The many-body calculations show that, although virtual-positronium is important, it is not the value of E_i (set by the weakest bound molecular electron) that determines the scale of enhancement, but rather interaction of the positron with all the possible molecular orbitals [4].

Thus, E_i by itself does not appear to determine the strength of the interaction. It is possible that, by separating molecules into classes with specific types of orbitals (e.g. different bonds and/or different substitutions), these effects could be studied systematically, but this will require additional experimental and theoretical work.

It is hard to see how one unifying picture using the global molecular parameters can describe the differences between isomer pairs. The one additional feature that does carry through is the effect of the geometry. For all comparisons between molecules with a substitution on the first carbon or the second carbon, the molecule with the substitution on the second carbon (i.e., nearer the center of the molecule) has a larger ε_B value. This includes butane and isobutane, although the effect is small. The importance of this effect is also seen in the dichloro-substituted propanes, where the 2,2-molecule with both carbons in the middle has an $\sim 50\%$ larger ε_B value than the 1,3-molecule (i.e. where the chlorines are split and attached to the ends). For these molecules, α , μ , and E_i are all very similar, and so the only remaining difference would appear to be the geometry. This has been observed in recent model calculations by Swann and Gribakin. Having the dipole in the middle of the molecule allows for the positron cloud to interact with more of the molecule. This, in turn, leads

to stronger binding and increased localization of the positron wave function [11].

An exception to this trend is the comparison of hexane to 2,3-dimethylbutane, which does not show a measurable change in ε_B . It could be that, for large molecules with little to no dipole moment, the extended nature of the attached state makes these isomeric differences less important [5]. Swann and Gribakin did find differences of 10 s of meV or more for certain hexane or heptane conformers [6], however entropic consideration lead to the predominance of only one or a few conformers in the annihilation spectra at 300 K. For the conformers, in contrast to the isomers studied here, the bonds are all the same, but the atomic groups are rotated with respect to the axis of the molecule. Since the lowest energy conformer is typically the chain with the atoms maximally separated, any conformational change should make the molecule more compact. In reference [6] Swann and Gribakin showed that the more compact shapes have increased ε_B . Similarly, a calculation of ε_B for a large number of conformers of hexadecane ($C_{16}H_{34}$) was done in reference [8]. Here they found a very large and complicated dependence on the exact shape of the conformer where the more compact forms generally also had higher calculated ε_B . It remains for future study to determine if similar differences in binding energy are present in other large alkane isomers and conformers, and whether evidence for these differences can be observed in the measured annihilation spectra.

4. Summary

Experiments have shown that most molecules can form positron bound states. The binding energies of these states can be determined using the measured resonant annihilation spectra as a function of incident positron energy. Using selected isomers, it has been shown that details of the molecular geometry can play an important role in setting the magnitude of ε_B . In most previous data-driven analyses (including our own), this dependence has been neglected, but was speculated to be a hidden parameter [17]. Here, by comparing specific isomers (i.e. where the geometry of the molecule is changed but not its constituents), it was possible to, at least partially, separate the effects of the global molecular parameters (i.e. which are approximately constant between isomers) and local changes in the molecular geometry. It is found that the molecule in the isomer pair in which the dipole (or polarizable center) is closer to the geometric center of the molecule has the larger value of ε_B . For molecules with small (or zero) dipole moment, this effect is seen to be small, whereas molecules with larger dipole moments exhibit larger changes, in some cases by as much as 50%.

These geometric effects are also apparent in recent theoretical work that used effective potential models combined with the full molecular geometry [10, 11]. The changes in ε_B predicted for different molecular conformers highlights the importance of molecular geometry [6, 9]. In particular, the changes in predicted ε_B for different molecular conformers highlighted the importance of molecular geometry [6, 8, 9]. These calculations showed that more compact molecular

structures generally have higher ε_B values. The *ab initio* many-body calculations of reference [4] observe a similar dependence on the shape of the molecule. In the framework of reference [4], the ‘geometrical effect’ described here also has contributions due to the differences in the individual molecular orbitals, including their individual ionization energies and other properties such as the anisotropic polarizability.

There is evidence that positron binding to aromatic molecules (e.g. benzene) and molecules with double or triple bonds is determined by additional effects [4, 8, 12]. This may be due to the fact that the stronger bonds localize more electrons inside the molecule and can lead to a strong polarizable center, the location of which can alter ε_B . Further, as seen in recent calculations, changing the type of bonds may cause important changes to the orbitals involved in virtual positronium, and this could have a large impact as well [4]. This could be part of the explanation as to why the small molecules acetylene and ethylene (with a triple C≡C bond and double C=C bond, respectively), have larger binding energies than the 2-carbon chain ethane [29]. Future measurements of more molecules with these types of bonds may enable a separation of these effects, similar to that done here for changes in geometry.

Acknowledgments

We thank G F Gribakin, A R Swann, J Hofierka and D G Green for many important conversations and suggestions related to the work presented here. This work supported by the National Science Foundation, Grant PHY-2010 699.

Data availability statement

The data that support the findings of this study are available upon reasonable request from the authors.

ORCID iDs

J R Danielson  <https://orcid.org/0000-0002-5904-7976>

S Ghosh  <https://orcid.org/0000-0003-2005-2943>

C M Surko  <https://orcid.org/0000-0001-9529-6956>

References

- [1] Gribakin G F, Young J A and Surko C M 2010 *Rev. Mod. Phys.* **82** 2557–607
- [2] Tachikawa M, Kita Y and Buenker R J 2011 *Phys. Chem. Chem. Phys.* **13** 2701
- [3] Tachikawa M, Kita Y and Buenker R J 2012 *New J. Phys.* **14** 035004
- [4] Hofierka J, Cunningham B, Rawlins C M, Patterson C H and Green D G 2021 arXiv:2105.06959
- [5] Swann A R and Gribakin G F 2019 *Phys. Rev. Lett.* **123** 113402
- [6] Swann A R and Gribakin G F 2020 *J. Chem. Phys.* **153** 184311
- [7] Swann A R and Gribakin G F 2020 *Phys. Rev. A* **101** 022702
- [8] Sugiura Y, Takayanagi T, Kita Y and Tachikawa M 2019 *Eur. Phys. J. D* **73** 162
- [9] Sugiura Y, Suzuki H, Otomo T, Miyazaki T, Takayanagi T and Tachikawa M 2020 *J. Comput. Chem.* **41** 1576
- [10] Suzuki H, Otomo T, Iida R, Sugiura Y, Takayanagi T and Tachikawa M 2020 *Phys. Rev. A* **102** 052830
- [11] Swann A R, Gribakin G F, Danielson J R, Ghosh S, Natisin M R and Surko C M 2021 *Phys. Rev. A* **104** 012813
- [12] Danielson J R, Young J A and Surko C M 2009 *J. Phys. B: At. Mol. Opt. Phys.* **42** 235203
- [13] Cheng X, Babikov D and Schrader D M 2011 *Phys. Rev. A* **83** 032504
- [14] Amaral P H R and Mohallem J R 2012 *Phys. Rev. A* **86** 042708
- [15] Gribakin G F and Swann A R 2015 *J. Phys. B: At. Mol. Opt. Phys.* **48** 215101
- [16] Amaral P H R and Mohallem J R 2020 *Phys. Rev. A* **102** 052808
- [17] Danielson J R, Jones A C L, Gosselin J J, Natisin M R and Surko C M 2012 *Phys. Rev. A* **85** 022709
- [18] Jones A C L, Danielson J R, Gosselin J J, Natisin M R and Surko C M 2012 *New J. Phys.* **14** 015006
- [19] Crawford O H 1971 *Mol. Phys.* **20** 585
- [20] Garrett W R 1978 *J. Chem. Phys.* **69** 2621
- [21] Desfrancois C, Grégoire G and Schermann J P 2004 *Few Body Syst.* **34** 169
- [22] Simons J 2008 *J. Phys. Chem. A* **112** 6401
- [23] Clary D C 1988 *J. Phys. Chem.* **92** 3173
- [24] Desfrancois C 1995 *Phys. Rev. A* **51** 3667
- [25] Desfrancois C, Abdoul-Carime H and Schermann J-P 1996 *Int. J. Mod. Phys. B* **10** 1339
- [26] Abdoul-Carime H and Desfrancois C 1998 *Eur. Phys. J. D* **2** 149
- [27] Hammer N I, Dirir K, Jordan K D, Desfrancois C and Compton R N 2003 *J. Chem. Phys.* **119** 3650
- [28] Danielson J R, Jones A C L, Natisin M R and Surko C M 2012 *Phys. Rev. Lett.* **109** 113201
- [29] Barnes L D, Gilbert S J and Surko C M 2003 *Phys. Rev. A* **67** 032706
- [30] Natisin M R, Danielson J R and Surko C M 2016 *Phys. Plasmas* **23** 023505
- [31] Murphy T J and Surko C M 1992 *Phys. Rev. A* **46** 5696
- [32] Danielson J R, Dubin D H E, Greaves R G and Surko C M 2015 *Rev. Mod. Phys.* **87** 247
- [33] Ghosh S, Danielson J R and Surko C M 2020 *J. Phys. B* **53** 085701
- [34] Gribakin G F and Lee C M R 2006 *Phys. Rev. Lett.* **97** 193201
- [35] Ghosh S, Danielson J R and Surko C M 2020 *Phys. Rev. Lett.* **125** 173401
- [36] NIST Mass Spectrometry Data Center Infrared spectra *NIST Chemistry WebBook* ed P J Linstrom and W G Mallard (*NIST Standard Reference Database No. 69*) (Gaithersburg, MD: National Institute of Standards and Technology) p 20899
- [37] Shimanouchi T 1972 *J. Phys. Chem. Ref. Data* **1** 189–216
- [38] Jones A C L, Danielson J R, Natisin M R and Surko C M 2013 *Phys. Rev. Lett.* **110** 223201
- [39] Gribakin G F, Stanton J F, Danielson J R, Natisin M R and Surko C M 2017 *Phys. Rev. A* **96** 062709
- [40] Young J A and Surko C M 2008 *Phys. Rev. A* **78** 032702
- [41] Danielson J R, Gosselin J J and Surko C M 2010 *Phys. Rev. Lett.* **104** 233201
- [42] Lide D R (ed) 2008–2009 *CRC Handbook of Chemistry and Physics* 89th edn (Boca Raton, FL: CRC Press)
- [43] Gussoni M, Rui M and Zerbi G 1998 *J. Mol. Struct.* **447** 163
- [44] Ha T-k, Pal C and Ghosh P N 1992 *Spectrochim. Acta A* **48** 1083
- [45] Mitroy J, Bromley M W J and Ryzhikh G G 2002 *J. Phys. B: At. Mol. Opt. Phys.* **35** R81
- [46] Mitroy J, Bromley M W J and Ryzhikh G 1999 *J. Phys. B: At. Mol. Opt. Phys.* **32** 2203